

THERMOHALINE OCEAN PROCESSES AND MODELS

J. A. Whitehead

Department of Physical Oceanography, Woods Hole Oceanographic
Institution, Woods Hole, Massachusetts 02543

KEY WORDS: thermal convection, salt convection, ocean circulation, buoyancy

INTRODUCTION

Understanding the physical behavior of the ocean is of interest to scientists in a variety of disciplines because ocean dynamics interacts with atmospheric processes to govern climatic and biological processes. For example, there is evidence that interactions between the ocean currents and temperature fields and the atmospheric temperature and wind fields are possible mechanisms for the El Niño-Southern Oscillation (ENSO) (Neelin, Latif & Jin 1994), which influences global weather fluctuations and biological production over periods of years. For longer time scales, climate record studies reveal numerous oscillations in $^{18}\text{O}/^{16}\text{O}$ ratios and foraminifera populations (Broecker et al 1985, Boyle 1990) which indicate that thermal and salinity distributions of past oceans differ significantly from the present ones.

Such observations are qualitatively consistent with a relatively new but very simple idea (Stommel 1961)—that the combined heat and evaporation boundary conditions imposed by the atmosphere can produce multiple states of ocean circulation. The states are thereby dependent on their initial condition. This causes them to exhibit catastrophic or discrete jumps as the boundary conditions are slowly varied owing to atmospheric changes. The governing equations are beautiful and simple examples of finite amplitude instability (also called catastrophic) transitions. Since records of the ice sheets indicate sudden melting and freezing events, it is

possible that such catastrophic jumps have been realized in ocean circulation in the past. This article explains and reviews the consequences of mixed boundary conditions of this type.

Even though this area of study has only recently been developed, there are already a number of summaries written about this problem. Each is presented in conjunction with oceanographic issues rather than with fluid mechanics itself. Each has also launched new interest in the area of the interplay between internal dynamics and boundary conditions. Following the initial suggestion that the ocean may have multiple states for the same boundary conditions, little additional interest is evident until Rooth (1982) discussed the role of temperature and salt in the buoyancy-driven component of the ocean circulation. He raised the possibility of a pole-to-pole circulation being generated for reasons similar to those raised by Stommel (1961). Welander (1986) fit the existing understanding of temperature and water flux boundary conditions into the context of ocean circulation and reviewed the numerous processes that can create time-dependent flows due to heat and salt effects. Weaver & Hughes (1992) produced an admirable and exhaustive review of the role of mixed boundary conditions from their use in simple box models to their influence on complex and sophisticated general circulation schemes. Marotzke (1994) summarized the development of box models and raised the question of even more feedback mechanisms from air-sea interaction. All of these summaries discuss the issues for the use of oceanographers, particularly those developing numerical models. This article gives a simplified and nonspecialized review for the general scientist interested in such possibilities.

THERMAL AND WIND-DRIVEN OCEAN—SCALING AND CONCEPTS

Although the influence of heat, mass, and momentum transport between ocean and atmosphere has been appreciated by oceanographers for decades, an understanding of their respective roles in forcing the ocean circulation is still being actively developed. The overall structure of the oceans is quite simple. From the equator to approximately 50 degrees latitude there is a surface layer less than 1 km deep of warm water in the “thermocline” where temperature ranges from 5°C up to 28°C. Wind-driven currents in the thermocline are some of the best-understood dynamic features in the oceans; they are westward in the tropics and eastward at mid-latitudes and in the same direction as the overhead winds. There are two particularly well-known types of confined intense boundary currents at the edge of the wind-driven currents. One type is the eastward flowing equatorial countercurrent that is found at depths of the order of

hundreds of meters at the equator. The other is the western boundary current such as the Gulf Stream, Kuroshio, etc. Both types of boundary currents arise because the Earth is a rotating sphere. In the southern ocean is a zonal Antarctic Circumpolar Current that is probably the deepest (most nearly barotropic) wind-driven current in all the oceans.

The thermocline encompasses the warmest water in the world but salinity of the thermocline water varies. It is highest in the tropics owing to high rates of evaporation, and lower in temperate zones. In the rest of the ocean, temperature decreases with latitude and depth, and salinity variations are also notable. In polar regions, surface layers of low salinity water are common.

There are a number of water masses that sink and spread out from known regions of origin within and below the thermocline. The spreading flows are usually characterized by strong currents along the western boundaries. The deep and bottom water in the oceans apparently sinks in small regions and spreads away with time scales of years to centuries. This water is densest because the water is coldest, yet salinity plays a key role; sinking happens only when and where low salinity surface water is absent.

The best understanding of circulation concerns the wind-driven ocean circulation, where notable developments were made by Ekman (1905, 1923), Sverdrup (1947), and Stommel (1948). They, by necessity, assumed a steady atmosphere that exerted wind stress on the ocean surface, and ignored the effects from heat and water flux. The overall balance of forces has wind exerting stress on the surface, producing an Ekman layer. This boundary layer produces water drift lateral to the wind from effects of Earth rotation. Variations in latitude or wind stress produce "Ekman pumping" that forces water vertically into and out of geostrophic currents below the Ekman layer. Only a small amount of vertical motion is needed to produce a large geostrophic velocity. The result is large wind-driven gyres circulating horizontally with smaller vertical motion. Over large ocean length scales the mass transport is quantified by the well known Sverdrup relation,

$$\beta v D = \text{curl } \tau, \quad (1)$$

which along with continuity $\partial u D / \partial x + (1 / \cos \phi) \partial v D \cos \phi / \partial y = 0$ and one boundary condition completely determines vertically averaged velocities u [in the westward (x) direction] and v [northward (y) direction]. Here D is the depth of penetration of the wind driving, β is the variation of the vertical component of the rotation vector with latitude, and τ is the wind stress. The gyres tend to be intensified in the west (Stommel 1966, Stern 1975, Gill 1982, Pedlosky 1987). These ideas were verified only crudely and qualitatively at first, but with time more precise quantitative veri-

fiction has come forth. For instance, verification of Ekman layer dynamics in the ocean was delayed for decades because of measurement complications from waves, temporal effects, and lateral advection effects. Even so, it was widely believed that the ocean boundary layers behave like Ekman layers, and such layers had been observed extensively in the laboratory.

Although thermal forcing was included in some of the early ocean circulation theories (Robinson & Stommel 1959, Welander 1959), only relatively inflexible similarity solutions to the governing differential equations were found. The solutions were informative, but they relied on custom-fitted surface boundary conditions—general problems could not be studied. Fuller understanding of the manner in which the wind and thermal conditions drive the oceanic flows has gradually emerged only through a number of studies that either invoke some theoretical approximation to allow solutions or make use of numerical methods. There have been numerous numerical models. Some of these are reported by Bryan (1968), Bryan & Cox (1968), Veronis (1973), Bryan et al (1975), and Bryan (1986). In general numerical models of the ocean concern the wind-driven motion. These have advanced to the point of providing special forecasting products, as described for instance in the series of 12 articles in *Oceanography*, volume 5, 1992. In such models, the ocean is represented as either a number of layers or levels. Heat, mass, and momentum flux between layers or levels is specified in various ways that are considered reasonable. Generally, vertical friction is set to a very small value (lateral friction is often much larger to eliminate numerical instabilities), mass flux between layers is zero or set to a prescribed constant value everywhere, and thermal conduction is set so that layer temperature is unchanging. Regions of bodily sinking of dense water might be imposed if required. The results impressively duplicate the wind-driven circulation in many regions of the world's oceans, and verify that the basic balances governing the wind-driven circulation are reliably understood. However, the thermally- and salinity-driven components of the circulation are less frequently studied.

In the early period of development of numerical studies, scaling considerations emerged that determined the depth of two portions of the thermocline (Bryan 1968, Bryan & Cox 1968, Veronis 1969, Welander 1971, Welander 1986, Bryan 1986). In all instances it is assumed that there is a geostrophic ocean governed by the thermal wind equation

$$\frac{fU}{D} = \frac{g\delta\rho}{\rho L}. \quad (2)$$

Here U is a geostrophic velocity which as before is assumed to be large at the surface and to drop off to zero at depth D , $\delta\rho$ is the vertical density

change which also is a function of depth D , L is a length equal to the size of an ocean basin, f is the Coriolis parameter, ρ is density, and g is gravity. If U is of order v (since the ocean gyres are approximately round) and if $\delta\rho$ is specified, D can be calculated by combining Equations (1) and (2)

$$D = \left(\frac{f\rho L \text{curl } \tau}{\beta g \delta\rho} \right)^{1/2}. \quad (3)$$

Using the approximation for Ekman suction $W_e = \tau/\rho fL$, and assuming that L is basin sized so that $\text{curl } \tau = \tau/L$, and $\beta = f/L$, this equation reduces to

$$D = \left(\frac{\rho W_e f L^2}{g \delta\rho} \right)^{1/2}. \quad (4)$$

This is the depth of the *advective* thermocline (Welander 1986), which is directly driven by Ekman pumping and usually is estimated to be some hundreds of meters deep. In this thermocline, thermal effects are passive except for the fact that the thermocline has lower density than fluid below it. Except for that, water at any temperature is advected wherever the wind directs. To a first approximation heat transfer from a water parcel to elsewhere happens only in the top or side boundary layers. It is not simple to investigate the role of the advective thermocline in the global heat transport until the transport into and out of the boundary layers on the top and to the west are known. However, progress has been made on the internal structure of this advective thermocline using layered models that need to fulfill certain requirements for solutions to be realized. Regions that cannot be penetrated by surface wind forcing (Luyten et al 1983) called "shadow zones," and regions where streamlines close so that potential vorticity becomes constant (Rhines & Young 1982) have been found. These have been identified with features in actual ocean regions. The governing dynamics is summarized by Pedlosky (1990).

The inertial thermocline is believed to lie above and equatorward to a larger and slower general circulation which involves buoyant sinking of denser water near the pole and rising of less dense water in temperate and equatorial regions. Conservation of heat in the upwelling regions is expressed by $W_h \partial T / \partial z = \kappa \partial^2 T / \partial z^2$, where κ is the thermal diffusivity and the upward velocity W_h is produced by the rising of cold water under the thermocline rather than by the wind. The source of this cold water is water that has sunk to great depths in polar regions. Scaling this relation by using an unknown thermocline depth D_h , so $W_h/D_h = \kappa/D_h^2$, and sub-

stituting W_h for W_c and D_h for D in (4), we find a depth of this thermocline to be

$$D_h \sim \left(\frac{\kappa f L^2 \rho}{g \delta \rho} \right)^{1/3}. \quad (5)$$

This derivation was found by Bryan & Cox (1968), Welander (1971, 1986), and Whitehead (1991), who also pointed out that this scaling is consistent with a heat transport from equatorial to polar regions of $\rho C_p (\kappa^2 L^4 g \alpha \Delta T^4 / 2f)^{1/3}$, where C_p is the specific heat of water. It is also derived in a salinity-driven context by Huang & Chou (1993).

LOCAL SINKING DYNAMICS

A body of fluid exposed to different temperatures at the top surface and insulated around the sides and bottom will exhibit markedly different behavior in the downwelling and upwelling regions. Fluid in the downwelling region must be warmer than the top boundary temperature. If it were colder, warmer water would continue to accumulate indefinitely at the top, since surface fluid converges over downwelling regions and low-density water cannot sink away. Thus a steady state can only be reached if the very coldest water in the body is located at the top boundary layer of the downwelling region. This water goes unstable, forming convection cells that efficiently transport the cold water down to the bottom. In contrast, in the upwelling regions cool water rises from the depths and is warmed by thermal conduction. Because the ocean is cooled by convection and warmed by conduction and is in approximately a steady state so that cooling equals heating, and because convection carries heat more easily than conduction, the convecting regions must be smaller than the conducting regions. A model that focused on the smallness of sinking regions was studied by Rossby (1965). The analysis of that model assumed two-dimensional viscous flow with a smoothly varying temperature imposed on the upper surface. The scaling of the equations was consistent with the notion that the sinking regions are smaller than the rising regions.

In fact, the sinking areas in the ocean also form episodically in time and are dependent on special preconditioning (Killworth 1983) that comes from ocean currents, basin shape, and climate factors such as severity of winters and water salinity considerations. Thus, exact relations that govern the ratio of areas and location of sinking are still being investigated. However, progress is probably dependent upon clarification of the thermal-haline problems that are the main topic of this review.

A simple scaling argument shows why the sinking region is small. Let

the heat transport by cooling be given by a convection cooling parameterization

$$H_c = \frac{0.1kA_1\Delta T}{d_o} \left(\frac{g\alpha\Delta T d_o^3}{\kappa\nu} \right)^{1/3} \quad (6)$$

[the coefficient and exponent are still only approximately known, and this approximation lies in the midst of many formulas that can be found in Siggia (1994)]. The conductive cooling at the base of the inertial thermocline is $H_h = kA_2\Delta T/D_h$. Here k is the thermal conductivity of water, A is area, ΔT is the temperature difference between the tropics and the freezing point of water, g is gravity, α is the coefficient of expansion, and d_o is the ocean depth in the polar region. Using Equation (5) for D_h , and setting $H_c = H_h$, we find that g , α , ΔT , and κ cancel out and the simple relation

$$0.1A_1 = A_2 \left(\frac{\nu}{fL^2} \right)^{1/3} \quad (7)$$

results. Using the molecular value of viscosity for water $\nu = 0.01 \text{ cm}^2\text{s}^{-1}$, $f = 10^{-4} \text{ s}^{-1}$, and $L = 10^4 \text{ km}$, the relation predicts that the ratio of surface area with conduction to convection area is immense—more than 10^4 . Given a typical ocean basin of size 10^4 km , the expected size of convection, or sinking regions is of order 100 km .

One other feature of thermal convection should be mentioned: the possibility of oscillations. It has been known that differentially heated thermal loops can produce oscillations. These arise because there can be a temporal phase lag between heat transfer and the buoyancy force. This lag is due to a spatial separation between regions where heat transfer and buoyancy forces happen. These oscillations have periods given by the distance traveled by a fluid parcel divided by the transit velocity. Welander (1986) listed a number of heat-salt oscillators with fluctuation times governed by the above time scales. The oscillations arise because there is a phase difference between the time the heat or salt is applied and the time the fluid is accelerated.

THERMOHALINE BOUNDARY CONDITIONS

The influence of salinity variations is obvious to oceanographers and takes high priority when the state of the oceans' water masses are discussed (Reid 1979). Yet to this point the influence of salt has hardly been mentioned because to a first approximation temperature seems to dominate the density that water will attain. In addition, the thermal problems outlined in

the last section possessed one unique state for each boundary condition, so that questions about the heat transport of the ocean seem easy to pose and solve. It was obvious as early as the 1960s that if the same questions were asked about a container with salt water that had boundary conditions appropriate for heat and evaporation, many equilibrium states could exist for the same boundary conditions. Few if any presentations of the basic dynamics of this problem are more comprehensible than Stommel's (1961) explanation of why there are many states possible. It is reviewed by many (Welander 1986, Marotzke 1989, Thual & McWilliams 1992) and is given again here in modified form.

Consider a mixed ocean basin of water initially at temperature T_0 being heated by thermal conduction to a reservoir (for instance the atmosphere) at temperature T_a . This boundary condition is frequently used for the ocean and is connected with the work of Haney (1971) that justified this relation. The basin is simultaneously evaporating at a constant rate E . (Stommel actually expressed salt flux as being governed by a diffusive law similar to the law of thermal conduction; we deviate in order to clarify the central role of the different boundary conditions for heat and salt in the physical description of the multiple states.) The equations for temperature and salinity are

$$\frac{\partial T}{\partial t} = K(T_a - T) \quad (8)$$

$$\frac{\partial S}{\partial t} = E, \quad (9)$$

and density is governed by the linearized equation of state

$$\rho = \rho_0(1 - \alpha T + \beta S), \quad (10)$$

where α and β are positive. The constant K expresses the heat exchange coefficient between ocean and atmosphere. It might be given for instance by $kA_i/dV\rho C_p$, where k is the thermal conductivity of air, A_i is the surface area of the ocean, d is the boundary layer thickness of the atmosphere, V is the volume of the ocean. However, it can be expressed by other combinations of parameters (for instance turbulent exchange coefficients) as well. The constant E expresses the effect of evaporation. It is equal to the volumetric rate of evaporation times salinity of the ocean divided by V . As with the temperature exchange coefficient, it can be expressed by other parameter groups as well.

The solution for Equations (8–10) is an exponential decay of temperature from T_0 to T_a , a linear increase in salinity with time, and, given a sufficient change in temperature, an initial decrease in density due to the

warming with a transition to an eventually steady increase with time from the increase in salinity. The evolution of T , S , and ρ is sketched in Figure 1a. Since density decreases then increases, there is a range of densities that have the same value at two different times. Moreover, density first becomes less than the original density, then it becomes greater than the original density.

Consider next the same basin with a steady inflow rate Q of water with temperature T_0 and salinity S_0 and an equal outflow with temperature T and salinity S . The equations governing T and S are

$$K(T_a - T) - Q(T - T_0) = 0 \quad (11)$$

$$E - Q(S - S_0) = 0 \quad (12)$$

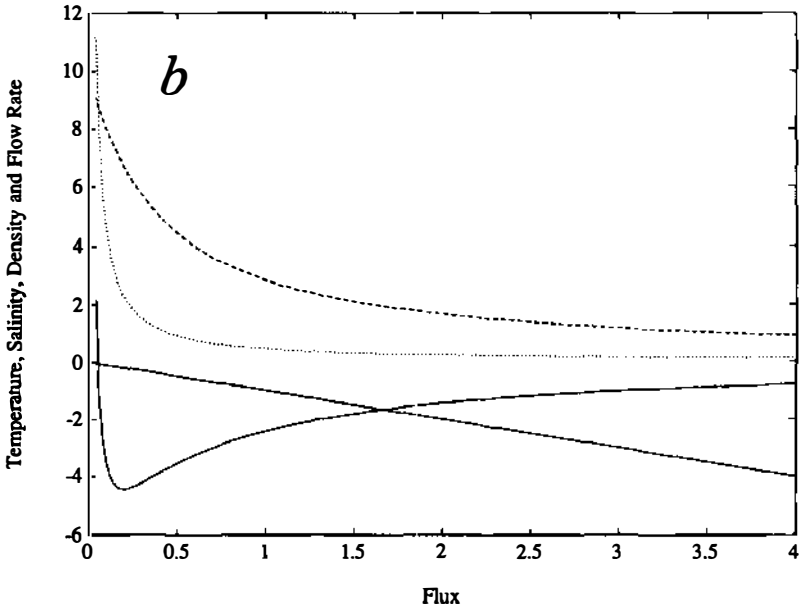
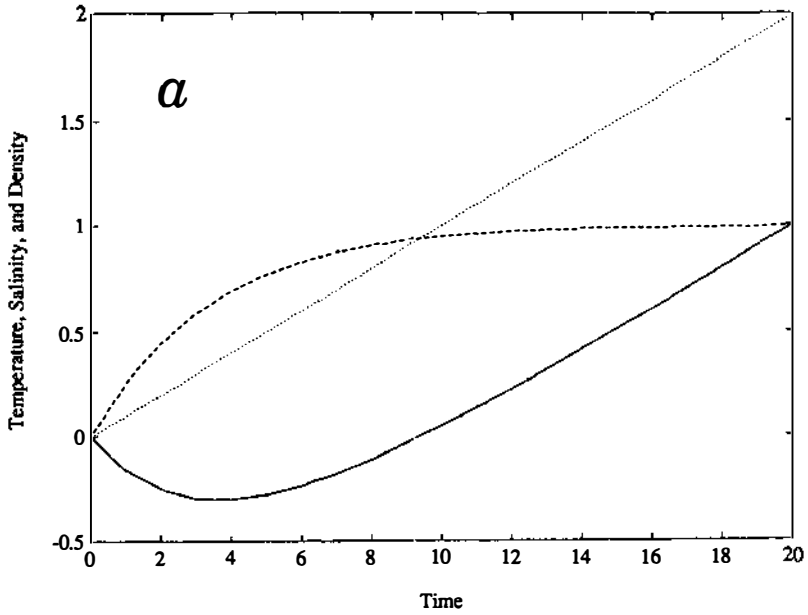
so

$$T = (KT_a + QT_0)/(Q + K) \quad (13)$$

$$S = S_0 + E/Q. \quad (14)$$

Figure 1b shows T , S , and ρ as functions of Q . The flow Q is roughly analogous to the inverse of time. Large Q decreases T from T_a and increases S above S_0 only slightly, whereas small Q decreases T more strongly, but even more greatly increases S and thereby ρ . As in the previous example, there is a range of densities that have the same value of density ρ at two different values of flux.

The final step in the illustration presents two oceans connected together by capillary pipes, one pipe at the surface and one at depth. Assume one ocean is exposed to positive temperature and evaporation and the other is exposed to exactly opposite values. Because of the pipes, each is subject to inflow of properties by the other, so $T_0 = -T$, $S_0 = -S$ can be substituted into Equations 11–14. The equations are identical to the equations with $T_0 = S_0 = 0$ except that E is doubled. The figures for T , S , and ρ versus Q are similar to those of Figure 1b because we set $T_0 = S_0 = 0$. If flux between the two oceans is driven by density difference, we assume the simplest possible relation between exchange flow rate Q and density difference between the two basins, i.e. Q is proportional to the density difference. Depending on the value of its slope, this line will intersect the curve of density versus Q at zero, one, or two points. For the case of intersection at one point, the coupled ocean basins are capable of only one T, S state, but for the case in which the line intersects the curve in two points, two states are possible. In many examples there are three states. Including the transient terms reveals that the two outside states are stable points in phase space and the intermediate one is an unstable saddle point.



There can be a spiraling trajectory into the stable point, in which case T, S would oscillate as the coupled ocean basins approached a stable state.

In practice it has been more common to consider the salt boundary condition to be diffusive in character in the box models (while freshwater flux is imposed in more realistic models). Following the notation by Thual & McWilliams, the complete time-dependent equations then read

$$\dot{\theta} = \alpha - \theta - |\Psi| \theta \quad (15)$$

$$\dot{\Sigma} = \beta - \xi \Sigma - |\Psi| \Sigma \quad (16)$$

$$\Psi = \theta - \Sigma, \quad (17)$$

where Ψ is the density difference between the two basins, θ is the temperature difference, and Σ is the salinity difference. The parameters that specify the system are $\xi = R_s/R_T$, where the R values are reciprocal time constants of salt and temperature respectively, and $\alpha = T_e - T_p$ and $\beta = \xi(S_e - S_p)$, where subscripts e and p stand for equator and pole, respectively. Steady flows are given for $\theta = \alpha/(1 + |\Psi|)$ and $\Sigma = \beta/(\xi + |\Psi|)$. The equation for Ψ is

$$\Psi(1 + |\Psi|)(\xi + |\Psi|) = \alpha(\xi + |\Psi|) - \beta(1 + |\Psi|). \quad (18)$$

Zero circulation implies $\Psi = 0$, so the above equation requires $\beta = \xi\alpha$. Thual & McWilliams showed that the domain of multiple states has a cusp-like structure on the α, β plane, starting at $\xi/(1 - \xi)$, $\xi^2(1 - \xi)$ and extending from the line $\beta = \xi\alpha$ to greater values of β that lie on a complicated cubic curve. The cusp is quadratic away from the intersection point rather than trending as $2/3$, as predicted for differential systems (Arnold 1984) because of the non-differentiability of the absolute value

Figure 1 Sketch of the behavior of temperature, salinity, and density for two simple boxes. (a) An isolated box with transient behavior (Equations 8–10). The constants used are $\alpha = \beta = 1$ and $k = 0.3$ with boundary conditions $T_a = 1$, $T_0 = 0$, and $E = 0.1$. Temperature (*dashed curve*) starts at zero and approaches the temperature of the “air.” The water is evaporating so salinity (*dotted line*) increases steadily with time. Density (*solid curve*) is salinity minus temperature. Near the beginning, it and has the same value at two different times. (b) A box with steady influx of water (Equations 10, 13, and 14). The constants used are $\alpha = \beta = 1$, $k = 0.1$ with boundary conditions $T_a = 10$, $T_0 = 0$, $S_0 = 0$, and $E = 0.45$. Temperature (*dashed curve*) is positive at small flux and goes to zero at large flux. Salinity (*dotted curve*) is very large at vanishing flux and zero at large flux. Density (*solid curve*) is positive at very small flux, but this decreases to a minimum as flux increases, then increases for still greater flux. Therefore, there is a range of flux where density has the same value for two different fluxes. If flux is buoyancy driven, it may be proportional to density (*solid straight line*). In this case, the solid line and curve cross at two points; thus two values of flux are possible for the same boundary conditions.

terms. For fixed salt flux in the box models there is no zero-circulation state since salt would increase indefinitely, so such an analysis cannot be made. Nevertheless, Thual & McWilliams were able to mimic the two-box model catastrophe range with a fluid model comprised of cells forced by surface temperature and salt flux boundary conditions, but in which diffusivity and nonlinear terms were present.

MULTIPLE BOX MODELS

There have been a large number of box model studies in recent years, not because the problems are simply more realistic, but because unexpected results have emerged and questions have arisen about how to deal with the new features. The configurations studied to date are schematically sketched in Figure 2.

A model with one equatorial box between two polar boxes is naturally the next simplest realization of the real oceans; it corresponds to a pole-to-pole ocean such as the Atlantic or Pacific. The model developed an unexpected collection of states. Obviously, it develops either symmetric flows with rising (or sinking) at the equator and sinking (or rising) at the pole, or nonsymmetric flows with weaker sinking (or rising) at one pole than at the other. In the extreme nonsymmetric case there is pole-to-pole circulation with rising at one pole, dense water preparation in the tropics, and sinking at the other pole. One can expect that the symmetric flows will possess the same features as the two box models reviewed above. The question is whether the nonsymmetric states will arise, and if so, what are their properties? The first multiple box variant to the original two-box model was originally suggested by Rooth (1982), who proposed a three-box model with only a direct connection of the return flow between the two poles. It was motivated by the fact that some oceans have more sinking in the polar regions than do others. Because there was no connection of the return flow with the equatorial box, this model was incapable of symmetric circulation. It was found that this model would develop an asymmetric flow. It was further suggested that this might happen in the actual ocean. Walin (1985), who was apparently unaware of the previous studies of this question, showed that a two-hemisphere model adopted asymmetric flow when in the thermal mode if the salt forcing was greater than one half the thermal forcing. Like Stommel's explanation, his explanation is simple enough to be included here in slightly modified form.

First, assume that volume flux is proportional to density difference between equator and pole. For a thermally driven pair of boxes, let volume flux $Q = -mT$, where m is a constant of proportionality. This simply says that surface circulation is away from the warm water and toward the cold

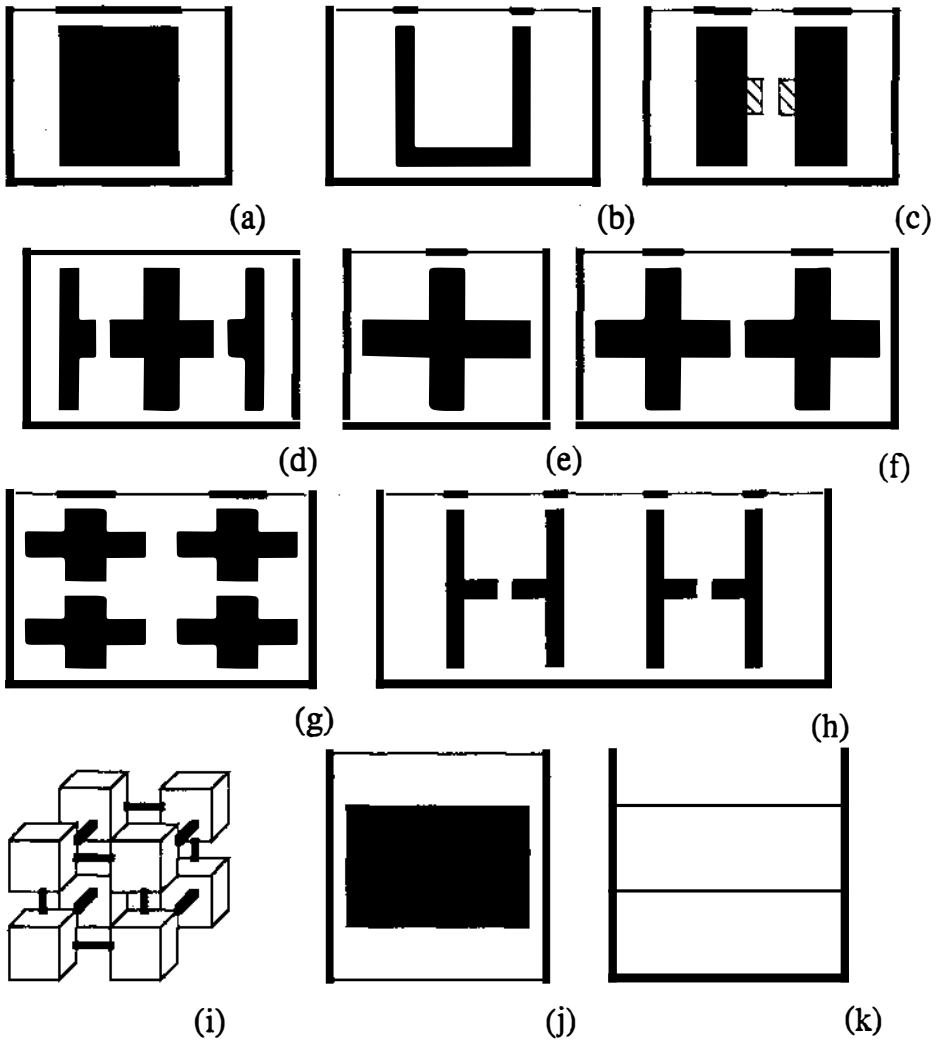


Figure 2 Sketch of the various box-model configurations that have been used to study the thermohaline problem. In all but the cube diagram (i), water is mixed in the large regions and flows through the narrow slots without mixing. Temperature and water can diffuse across thin lines but not across thick lines. (a) Stommel (1961), (b) Rooth (1982), (c) Walin (1985), Welander (1986), and (Joyce 1991) (with a separation barrier as shown with cross hatches between deep and surface boxes to produce a deep abyssal basin), (d) Marotzke (1989), (e) Huang et al (1992), (f) Huang & Stommel (1992), (g) Kagan & Maslova (1990), (h) Marotzke (1989, 1990), (i) Huang & Stommel (1992), (j) Keller, (1966), Welander (1967), Dewar & Huang (1994), (k) Welander (1982).

water. In addition, let normalized heat flux H [heat flux/(density times specific heat)] be $H = QT$. Now consider a three-box pole-to-equator-to-pole model with both boxes having the above steady balance between the symmetric temperature T , Q , and H . Let T' be a deviation from symmetry. The equation governing an antisymmetric perturbation is $T'_t = (Q + Q')(T + T') - QT = -2mTT'$ for small T' . This has a decaying solution. Consider combined thermal forcing with salt forcing so salt is added to the equator and taken away at the poles. The flux of salt is $F_s = QS$; where the volume flux Q is proportional to the density difference $Q = -mT + jS$. Thus, surface flux is away from warm water but toward salty water. Assume for simplicity that the system is forced to retain symmetric temperature. The equation governing the antisymmetric salt perturbation is $S'_t = (Q + Q')(S + S') - QS = (-mT + 2jS)S'$. For $2jS > mT$, the term in parentheses is positive so the perturbation will grow exponentially and the antisymmetric solution will be present.

It is useful to review our understanding to this point. For the two-box model, there can be either a state with one value of circulation for the given boundary conditions or multiple states with many values of circulation for exactly the same values of given boundary conditions. If there are three values, two states are stable and one is unstable. The multiple states are only found when the forces of buoyancy from temperature and salinity oppose each other. They are most commonly found when the opposing forces are roughly of comparable magnitude.

With three boxes, corresponding to basins with a pole-equator-pole configuration, there can be either states with purely symmetric rising or sinking at the equator, or (more commonly) there can be nonsymmetric states, with stronger circulation between equator and one pole than the other. As in the two-box case, the antisymmetric state develops when temperature and salinity oppose each other and are of comparable magnitude.

The transition from symmetric to antisymmetric circulation was found by Bryan (1986) using a general circulation model. Such models use finite-difference equations to solve approximations to the Navier-Stokes equations in a number of coupled layers or depths. The transition was triggered by starting an experimental run, which previously was found to be symmetric, with a negative salinity anomaly of 0.1‰ poleward of 45° in the southern hemisphere. The freshening caused the deep convection to cease, thereby increasing the residence time of the waters near the south pole. This caused the water to become even fresher because of precipitation in that region; thus the anomaly increased. It was also noted that in the asymmetric case, the poleward heat transport was also asymmetric. In fact, there was transport of heat toward the equator over most of the

southern hemisphere, a cross equatorial heat flux of the same magnitude as the maximum transport for the symmetric case, and approximately twice the transport in the northern hemisphere. This effect could of course lead to different climates in the two hemispheres. Owing to the complexity of the general circulation model, it was not possible to isolate the cause of the transition in the model and many other factors were suggested to play a role as well.

The pole-to-pole circulation was also found in numerical studies of convective flows by Marotzke et al (1989) (also in Marotzke 1990). In these studies the two-dimensional low Reynolds number flow in a box subjected to heating and freshwater flux on the upper boundary was numerically solved. Boundary conditions were imposed that were symmetric about the equator. In spite of this, the asymmetric flow was obtained if a large enough temporary asymmetric perturbation was imposed. Considerable discussion was given concerning effects in the convective adjustment region, where density is inverted. These effects lead to highly focused downwelling regions (as scaled perhaps by our Equation 7) and actual density inversions. Such inversions would not be found in geophysical systems because convection would be expected. The inversion is often removed artificially by setting density constant with depth and calculating a surface maximum subject to the constraint of vertical conservation of heat. It was asked whether the convective adjustment was a cause of the asymmetry. However, the asymmetry was found whether or not the convective adjustment mechanism was imposed. This is consistent with the notion that the asymmetry was not caused by the convective adjustment but was consistent with multiple states arising from different boundary conditions as reviewed here.

It was also pointed out that the pole-to-pole circulation transports heat toward the polar region that has sinking water, and away from the polar region with upwelling. This fact is not only important for climate considerations, but is observed to happen in the South Atlantic.

In the following years analyses were extended to a variety of multiple-box models by Welander (1989), Birchfield (1989), Marotzke (1989), Kagan & Maslova (1990), Joyce (1991), Huang et al (1992), Huang & Stommel (1992), and Thual & McWilliams (1992). Many of the configurations corresponding to these models are sketched in Figure 2. Welander showed that the steady flows of three or more box models can be represented as the superposition of two-box model steady solutions. The solutions with symmetric rising or sinking at the equator were difficult to produce and were only recovered by imposing symmetry about the equator. Thual & McWilliams verified the superposition principle found by Welander, but only for small values of a governing parameter. In

the more general case, there is no known superposition principle. A robustness of the pole-to-pole circulation was found within a symmetric cusp.

Kagan & Maslova (1990) considered the number of modes and their general stability properties for a 3×3 pole-equator-pole situation. They found that numerous modes were locally stable and that the state function is a global Lyapunov function, so that there is no limit to cycle oscillations.

Birchfield (1989), Birchfield et al (1990), and Joyce (1991) included a bottom box that represented abyssal waters. This inclusion is motivated partly because the abyssal waters can be directly observed, with their fluxes in the ocean monitored, and because there is some understanding of the relations between their flux and bottom geometric factors. Joyce found that the inclusion led to a long-term quasi-periodic oscillation when bottom water formation was inhibited.

Huang et al (1992) investigated boxes that were stacked in the vertical as well as connected horizontally in arrays of 2×2 and 3×2 . The 2×2 arrangement allows for a change in density with depth as well as with latitude. Since only advection was included, the change in density of the bottom cells occurs only because of unequal temperatures between the box and the box feeding into it. In the case when either mode is possible, the probability of being in one mode or the other from random initial conditions was calculated. A Monte Carlo scheme was used to integrate the equations from random initial temperatures between 0 to 25°C and from 31.5 to 38.5 salinity units. It was found that for precipitation rates, and parameters of the present-day North Atlantic, the possibility of being in the thermal mode is roughly 30% but there is a sharp increase in probability for the saline mode at slightly larger values of precipitation. At only 20% greater precipitation the saline mode is 100% probable.

The 3×2 box models were designed to analyze the question of intermediate water formation, and had vertically stacked pairs of boxes representing polar, temperate, and equatorial ocean. The calculations showed that there were many minor modes that could exist but were generally statistically improbable. The “grand thermal mode” and the “grand saline mode” were found to continue to be prevalent and most common. However, because the present thermohaline circulation is close to a critical state in which a small increase in salinity would cause a departure from the present thermally dominated state, a shallower mode would result in sluggish motion in the polar regions and strong sinking at mid-latitudes.

Wind stress has been included in a $2 \times 2 \times 2$ box model (Huang & Stommel 1992), and results are generally similar to the 2×2 model above. The catastrophe is divided into several modes, but only a few of these modes are sizable. Again with parameters appropriate for the North Atlan-

tic, the thermal circulation is predicted. It takes three times more precipitation to transform to the saline mode in this case. Since the above 2×2 box model only required 20% for precipitation to transform to the saline mode, the results highlight the important role of rotation in the actual quantitative thermohaline balances.

Huang & Stommel's (1992) paper presented the results of calculations involving the well-known hysteresis loop (Figure 3) in a novel (to this author) and useful way. Although there are regions in solution space that can have more than one solution, the final state is easily calculated if the forcing parameter is systematically varied. Figure 4 sketches a fanciful map of the final states for two cases, one where the forcing parameter E is increased gradually, and another where it is decreased. Such maps were presented by Huang & Stommel so that the reader could visualize the extent of the hysteresis effects. This is a very useful visualization aid for such nonlinear problems.

MORE COMPLICATED OCEAN MODELS

There are of course numerous models of ocean circulation of more complexity than the simple box models. The simplest models beyond the box models utilize some simplifying assumption about the flow field. Amplitude equations allow a direct analysis of the evolution of the salinity field. These have been developed by Cessi & Young (1992) using a depth-averaged shallow ocean approximation (in which vertical diffusion balances lateral advection so that lateral velocity profiles are simple polynomials). They find a governing equation for depth-averaged salinity S of the form

$$\partial_t S = \kappa_s \partial_y^2 S + c \left(\frac{d^8 g^2}{v^2 \kappa_s} \right) \partial_y [(\alpha_s \partial_y S - \alpha_T \partial_y T)^2 \partial_y S] + \left(\frac{\kappa_s \Delta S}{d^2} \right) F(y), \quad (19)$$

where c is a dimensionless constant determined by the boundary

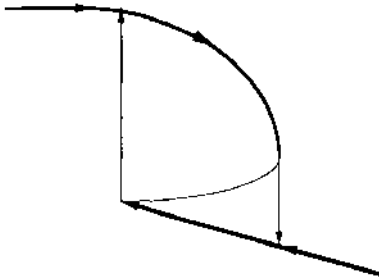


Figure 3 Sketch of the transition-hysteresis curve of a finite amplitude instability.

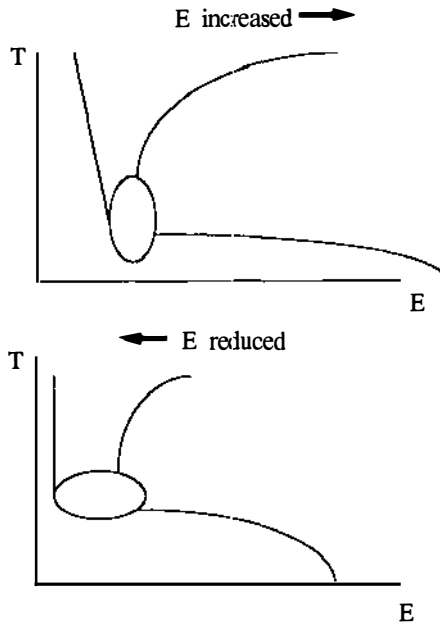


Figure 4 Sketch of stability regions that were shown by Huang & Stommel (1992). Since this is meant to represent realizable regions for a system with hysteresis curves, the regions depend on the way the parameters T and E change. For instance, the regions might differ as sketched depending on whether E decreases or increases for fixed T .

conditions, $F(y)$ is the salt flux forcing, T follows the temperature forcing (both imposed at the top surface), d is the depth of the ocean, g is gravity, ν is viscosity, and the other variables are as given previously. Subscripts T and S denote temperature and salinity, respectively. The terms represent, from left to right, change in salinity with time, lateral diffusion, lateral advection by the velocity, and surface flux forcing. In some parameter spaces this equation has three or more equilibria, some stable and some unstable. In the simplest case it also has a Lyapunov functional whose variational expression permits a simplified view of the stability of the various solutions. In particular, the globally minimum solution is identified, which will be realized if all solutions are subjected to large localized perturbations. Based on this concept, Cessi & Young identify regions where local minima are most vulnerable to perturbations, and other regions where they should be relatively invulnerable. At present, such vulnerability has not been checked in general circulation models.

Most analyses have been conducted for forcing that represents one pole-to-pole ocean. As in the box models the forcing that is symmetric about

the equator has both symmetric and asymmetric solutions, and both are locally stable. The symmetric solution possesses two cells of equal strength with sinking either at the pole from cooling or at the equator from salt flux. The asymmetric solution possesses two cells of different strength with a separating streamline at the equator rather than one cell from pole to pole as found in the numerical studies of Thual & McWilliams (1992). In addition, this type of solution has only one cusp catastrophe rather than the two found by them.

A zonally averaged ocean model has two-dimensional motion but incorporates some simplified effects of rotation without including the complexities of the entire three-dimensional wind-driven flows. Marotzke et al (1989) developed such an ocean model. Its strength over the box models is that it includes resolution of numerous depths and latitudes. It was found that the symmetric circulation was produced when surface salinity was specified, but that the symmetric circulation was unstable and the pole-to-pole circulation was stable under mixed flux-type boundary conditions. Flows in which there is symmetrical rising or sinking about the equator were only recovered when that symmetry was imposed. In addition, since the model now has many degrees of freedom, the evolution with time is considerably more complicated than the evolution of the simple box models. Marotzke (1989) used the same model as above to find that the salt-driven mode slowly changed and ultimately collapsed to a thermally-driven mode. Wright & Stocker (1991) used a slightly different model, which also slowly drifted with time while in the saline mode. They observed two drift-collapse episodes over a modeled time of over 50,000 years. They point out that both the boundary conditions and the values of diffusion in the interior of the domain have important effects on the evolution of the interior state. Since processes that govern interior diffusion are still being studied, it is difficult to know how to pick the parameters that express this diffusion precisely. Because such parameters may affect both qualitative behavior (such as catastrophic transitions) and quantitative behavior (such as drift rates), the models are very useful indicators but not yet predictive tools.

Such zonally averaged models can also incorporate many basins and so represent either hemispheric or global geometries. Stocker & Wright (1991) adopted a global geometry consisting of two oceans extending to the northern hemisphere and connected in the southern hemisphere. In their model that starts with boundary conditions that restore salinity and temperature to surface values, and which used the same values for both oceans, two-cell structures were produced on both basins. When this model was transformed to a model with mixed boundary conditions (the temperature

condition was the same but a salt flux boundary condition was imposed) the model adopted a flow with sinking in the northern extent of both basins. In contrast, with the realistic case of different values of surface salinity imposed in the Atlantic and Pacific there was a surface flow to the north in the Atlantic, with sinking in the north, and a surface flow to the south in the Pacific, with sinking in the south. Transforming to mixed boundary conditions from this state resulted in no qualitative change. Therefore, Stocker & Wright were able to produce the “oceanic conveyor belt” of strong sinking in the North Atlantic, which was originally proposed by Gordon (1986) [but is mentioned earlier in many articles such as those by Rooth (1982) and Walin (1985)] and is now widely accepted as happening in the present oceans.

Stocker & Wright were also able to produce two different end states for the same driving conditions but with different values of initial surface salinity, as many models had done before. They used values of anomaly corresponding to two different estimates of freshwater flux after the last ice age and recovered either no interocean exchange or the original conveyor belt.

Larger numerical models have documented the thermohaline transitions in greater detail. Weaver & Sarachik (1990) have seen such transitions in a one-hemisphere, 12-level model and a two-hemisphere 33-layer model. In the two-hemisphere model there are many stages of violent change separated by periods of gradual adjustment that are hundreds of years long. In the hemispheric model, oscillations with decadal time scales are identified with movement of salinity anomalies into convection regions. After a period of such oscillations, a transition to an overturning flushing mode is seen. The ocean then quiets down to either a deep convection mode or a quiet “collapsed” state.

Discussion about the dependence of the results on numerical schemes indicates that the transitions are sensitive to those parameters just as they are to the physical parameters. It is central in these problems that actual jump points in catastrophic transitions depend on a delicate balance between large quantities. Thus the transitions are naturally very sensitive to numerical effects.

Although numerous general circulation models simply impose a surface salinity, recent models have incorporated the influences of both temperature and freshwater flux forcing in some form. Most of the more recent numerical models specify either a salinity relaxation boundary condition or a salt flux condition. Weaver & Sarachik (1990, 1991) also point out that many numerical projects use adjusted flux conditions. Since it is more efficient numerically to specify salinity than flux, they impose

salinity then determine flux, and adjust salinity until the desired flux is obtained.

But the salt flux condition itself is only a convenient approximation; our original example used the oceanographically more correct water flux boundary condition. This correct condition was used by Marotzke & Willebrand (1991) in a primitive equation general circulation model. Four stable states for the same boundary conditions were found for a model with identical pole-to-pole basins connected by a circumpolar channel. The model incorporated wind forcing and utilized 15 vertical layers. It differed from the above by being driven by water flux rather than salt flux, by having a circumpolar connection between the Atlantic and Pacific, and by having Atlantic and Pacific oceans of the same size. In their results, two states have the oceans with identical circulation with sinking either in the north or south. The other two have sinking in the north in one basin and in the south in the other. The amount of change of freshwater flux needed to produce a transition from one state to another was found to be "modest," or significantly less than total flux. Tziperman et al (1994) closely examine the effect of the boundary conditions in close proximity to the transition point. Their motivation is, in part, to see how the instability "can be avoided," which is curious since it is a real physical effect and not a numerical instability.

Recently, other effects from a water flux boundary condition have been discovered. Huang (1993) has developed the freshwater flux boundary conditions for primitive equation circulation models, so that the use of a relaxation condition for imposing salt flux is unnecessary. The general circulation model by Huang & Chou (1993), which naturally includes the effects of rotation, was driven by evaporation and precipitation forcing alone. This model exhibits periodic and chaotic time fluctuations. The time dependence is due principally to the evaporation/precipitation boundary conditions. In addition to altering the surface salinity of the water, the freshwater flux produces large flows from small amounts of vortex stretching. This circulation, called the Goldsborough circulation (Goldsborough 1933, Huang & Schmitt 1993), produced effects similar to wind pumping of the Ekman layer. Thermally- or salt-flux-driven models of the same type would possess only steady flows because the stretching is absent, but it was not clear whether steady wind driving would produce the same time-dependent effect.

A systematic study of a general circulation model that includes the effect of evaporation and precipitation, and thermal and wind forcing, has recently been completed by Huang (1994). All computations were conducted for a pole-to-equator basin. It is pointed out that although the

time scale for temperature change is of the order of 43 days, for salinity it is tens of years. As in the box models, this difference provides the mechanism for the dual state of temperature and salinity forcing. Also as in the box models, below a critical rate of evaporation there is a thermal mode with sinking in the north. Above the critical rate, the ocean adopts a saline mode. However, this mode has different behavior from those of the box models because the saline mode continuously changes and suddenly reverts to a more vigorous thermal mode. Even though wind-driven circulation is superimposed in this model, the slow evolution of the salt-driven mode to an ultimate catastrophic transition to a thermal mode is very similar to the evolution seen by Marotzke (1989). During the saline mode the intermediate and deep water gets warmer and saltier. Above the salty water is a layer of fresh water that continually gets shallower. Finally, a cooling outbreak happens and the warm salty water becomes cooled and extremely dense, and this triggers the thermal phase, whose downward convection is strengthened by the fact that the deep waters have become very warm during the salt-driven phase. After some time it changes back to the saline mode, in agreement with the results of Stocker & Wright (1991). For parameters appropriate for the North Atlantic, the time scale for the entire cycle is hundreds of years. It was also noted that there is stronger sinking along the equator for no wind stress, but weaker sinking to mid depths with wind stress.

APPLICATION TO OTHER PROBLEMS AND SUMMARY

A theoretical model of a mixed layer in the ocean with differing heat flux and salinity flux boundary conditions has been found to develop growing oscillations from processes similar to those described above (Welander 1982). In this model, there is a well-mixed layer within which a turbulent exchange of heat and salt takes place, and the underlying water is of constant density. The oscillations are driven by a difference in the thermal relaxation time between the temperature and salt. The oscillations are also influenced by the fact that the exchange between the layer and the lower fluid is a function of the density difference between the layer and the deep fluid. This produces phase lags in the temperature and salinity fluctuations which can produce growing fluctuations.

Welander (1989) has also found an instability of a layer of fluid with top boundary conditions of constant temperature and constant freshwater flux. Oscillations grow because the salinity and temperature enter the fluid at differing rates owing to the two kinds of boundary conditions. These produce a phase lag between the density fluctuation and the buoyancy

force that can result in growing oscillations. This instability happens even if the internal diffusivity of heat and salt are the same, which may be true in the ocean because turbulent stirring is thought to mix both heat and salinity. The growth of the oscillation is not surprising because phase lags between density fluctuations and the buoyancy force also produce oscillations in simple models of convection cells (Keller 1966, Welander 1967) and in double diffusion (as reviewed by Schmitt 1994). However, in each case the values of the phase lags must be determined before one can find whether the oscillations will grow, decay, or remain neutral. Most recently, W. Dewar & R. X. Huang (private communication) have predicted growing oscillations of a simple loop model forced by freshwater flux.

In estuaries and on continental shelves, both temperature and salinity factors are important in determining the water circulation. Yet little interest has been expressed by coastal oceanographers to date. Moreover, river runoff is clearly similar to a specified flux condition whereas water temperature follows temperature of the atmosphere so that it remains determined by a relaxation condition. Therefore, there may be numerous examples of the phenomena reviewed here in shelves and estuaries. In addition, since the salinity and temperature of coastal water affect biological processes, there must be a wealth of ecological implications for these processes. It will be interesting to see if this unexplored area is opened in the future.

The most significant effect of the multiple states on the climate is that the equator-to-pole heat transport of the ocean depends not only on the boundary conditions that the atmosphere exerts on the ocean but on the initial state of the ocean as well. Thus a past ocean could possibly possess two or more different states and hence different values of heat transport even with the same atmospheric climate. This is going to make the duplication of past climates or the prediction of future climates extremely challenging. In addition, the jumps from one state to another will introduce frequencies that have nothing to do with the forcing frequencies of the boxes. This will further confuse the interpretation of historical data.

Ironically, although advances in most areas of fluid mechanics and in particular in the areas of convection and double diffusion (which are the closest to this new area of understanding) have been made using laboratory studies and analytical theory, all progress to date in this area has utilized only analyses or numerical studies. Not one laboratory study has been conducted nor one example directly observed in nature with the significant exception of the great conveyor belt concept. It will be interesting to see if new phenomena are found when the processes described here are sought in actual physical systems.

Any *Annual Review* chapter, as well as any article cited in an *Annual Review* chapter, may be purchased from the Annual Reviews Preprints and Reprints service.
1-800-347-8007; 415-259-5017; email: arpr@class.org

Literature Cited

- Arnold VI. 1984. *Catastrophe Theory*. New York: Springer-Verlag
- Birchfield GE. 1989. A coupled ocean-atmosphere climate model: temperature versus salinity effect on the thermohaline circulation. *Climate Dyn.* 4: 57-71
- Birchfield EG, Wang H, Wyant M. 1990. A bi-modal climate response controlled by water vapor in a coupled ocean-atmosphere box model. *Paleoceanography* 5: 383-95
- Boyle EA. 1990. Quaternary deepwater paleoceanography. *Science* 249: 863-70
- Broecker WS, Peteet DM, Rind D. 1985. Does the ocean-atmosphere system have more than one stable mode of operation? *Nature* 315: 21-26
- Bryan F. 1986. High-latitude salinity effects and interhemispheric thermohaline circulations. *Nature* 323: 301-4
- Bryan K. 1968. A non-linear model of an ocean driven by wind and differential heating. Part I, Description of the three-velocity and temperature fields. *J. Atmos. Sci.* 25: 945-67
- Bryan K, Cox MD. 1968. A non-linear model of an ocean driven by wind and differential heating, Parts I and II. *J. Atmos. Sci.* 25: 945-78
- Bryan KS, Manabe S, Pacanowski RC. 1975. A global ocean-atmosphere climate model, Part II. The oceanic circulation. *J. Phys. Oceanogr.* 5: 30-46
- Cessi P, Young WR. 1992. Multiple equilibria in two-dimensional thermohaline circulation. *J. Fluid Mech.* 241: 291-309
- Ekman VW. 1905. On the influence of the earth's rotation on ocean currents. *Ark. Mat. Astron. Fys.* 11: 52
- Ekman VW. 1923. Ueber Horizontalzirkulation bei winderzeugten Meeresströmungen. *Ark. Mat. Astron. Fys.* 17: 74
- Gill AE. 1982. *Atmosphere-Ocean Dynamics*. New York: Academic. 662 pp.
- Goldsborough GR. 1933. Ocean currents produced by evaporation and precipitation. *Proc. R. Soc. London Ser. A* 141: 512-17
- Gordon AL. 1986. Interocean exchange of thermocline water. *J. Geophys. Res.* 91: 5037-46
- Haney RL. 1971. Surface thermal boundary condition for ocean circulation models. *J. Phys. Oceanogr.* 1: 241-48
- Huang RX. 1993. Real freshwater flux as a natural boundary condition for the salinity balance and thermohaline circulation forced by evaporation and precipitation. *J. Phys. Oceanogr.* 23: 2428-46
- Huang RX. 1994. Thermohaline circulation: energetics and variability in a single-hemisphere basin model. *J. Geophys. Res.* In press
- Huang RX, Chou RL. 1993. Parameter sensitivity study of the saline circulation. *Climate Dyn.* 175: 1-18
- Huang RX, Luyten JR, Stommel HM. 1992. Multiple equilibrium states in combined thermal and saline circulation. *J. Phys. Oceanogr.* 22: 231-46
- Huang RX, Schmitt RW. 1993. The Goldsbrough-Stommel circulation of the World Oceans. *J. Phys. Oceanogr.* 23: 1277-84
- Huang RX, Stommel HM. 1992. Convective flow patterns in an eight-box cube driven by combined wind stress, thermal and saline forcing. *J. Geophys. Res.* 97: 2347-64
- Joyce TM. 1991. Thermohaline catastrophe in a simple four-box model of the ocean climate. *J. Geophys. Res.* 96: 20,393-402
- Kagan BA, Maslova NB. 1990. Multiple equilibria of the thermohaline circulation in a ventilated ocean model. *Ocean Modelling* 90: 9-24
- Keller JB. 1966. Periodic oscillations in a model of thermal convection. *J. Fluid Mech.* 26: 599-606
- Killworth PD. 1983. Deep convection in the world oceans. *Rev. Geophys. Space Phys.* 21: 1-26
- Luyten JR, Pedlosky J, Stommel H. 1983. The ventilated thermocline. *J. Phys. Oceanogr.* 13: 292-309
- Marotzke J. 1989. Instabilities and multiple steady states of the thermohaline circulation. In *Oceanic Circulation Models: Combining Data and Dynamics*, ed. DLT Anderson, J Willebrand, pp. 501-11. Dordrecht: Kluwer
- Marotzke A. 1990. *Instabilities and multiple equilibria of the thermohaline circulation*. PhD thesis. Inst. Meerskund, Univ. Keil, Germany. 126 pp.

- Marotzke J. 1994. Ocean models in climate problems. In *Ocean Processes in Climate Dynamics: Global and Mediterranean Examples*, ed. P. Malanotte-Rizzole, AR Robinson, pp. 79–109. Dordrecht: Kluwer
- Marotzke J, Welander P, Willebrand J. 1988. Instability and multiple steady states in a meridional-plane model of the thermohaline circulation. *Tellus* 40A: 162–72
- Marotzke J, Willebrand J. 1991. Multiple equilibria of the global thermohaline circulation. *J. Phys. Oceanogr.* 21: 1372–84
- Neelin JD, Latif M, Jin FF. 1994. Dynamics of coupled ocean-atmosphere models: the tropical problem. *Annu. Rev. Fluid Mech.* 26: 617–59
- Pedlosky J. 1987. *Geophysical Fluid Dynamics*. New York: Springer-Verlag. 710 pp. 2nd ed.
- Pedlosky J. 1990. The dynamics of the oceanic subtropical gyres. *Science* 248: 316–22
- Reid J. 1979. On the contribution of the Mediterranean Sea outflow to the Norwegian-Greenland Sea. *Deep-Sea Res.* 19: 1199–223
- Rhines P, Young W. 1982. A theory of the wind-driven circulation. I. Mid-ocean gyres. *J. Mar. Res.* 40: 559–96
- Robinson AR, Stommel H. 1959. The oceanic thermocline and the associated thermohaline circulation. *Tellus* 11: 295–308
- Rooth C. 1982. Hydrology and ocean circulation. *Prog. Oceanogr.* 11: 131–49
- Rossby HT. 1965. On thermal convection driven by non-uniform heating from below: an experimental study. *Deep-Sea Res.* 12: 9–16
- Schmitt RW. 1994. Double diffusion in oceanography. *Annu. Rev. Fluid Mech.* 26: 255–85
- Siggia ED. 1994. High Rayleigh number convection. *Annu. Rev. Fluid Mech.* 26: 137–68
- Stern M. 1975. *Ocean Circulation Physics*. New York: Academic. 246 pp.
- Stocker TF, Wright DG. 1991. A zonally averaged ocean model for the thermohaline circulation, Part II: Inter-ocean circulation in the Pacific-Atlantic basin system. *J. Phys. Oceanogr.* 21: 1725–39
- Stommel H. 1948. The western intensification of wind-driven currents. *Trans. Am. Geophys. Union* 29: 202–6
- Stommel H. 1961. Thermohaline convection with two stable regimes of flow. *Tellus* 13: 224–30
- Stommel H. 1966. *The Gulf Stream*. Berkeley: Univ. Calif. Press. 248 pp. 2nd ed.
- Sverdrup H. 1947. Wind-driven currents in a baroclinic ocean; with application to the equatorial currents of the eastern Pacific. *Proc. Natl. Acad. Sci. USA* 33: 318–26
- Thual O, McWilliams JC. 1992. The catastrophe structure of thermohaline convection in a two-dimensional fluid model and a comparison with low-order box models. *Geophys. Astrophys. Fluid Dyn.* 64: 67–95
- Tziperman E, Toggweiler JR, Feliks Y, Bryan K. 1994. Instability of the thermohaline circulation with respect to mixed boundary conditions: is it really a problem for realistic models? *J. Phys. Oceanogr.* 24: 217–32
- Veronis G. 1969. On theoretical models of the thermocline circulation. *Deep-Sea Res.* 16: 301–23
- Veronis G. 1973. Large scale ocean circulation. *Adv. Appl. Mech.* 13: 1–92
- Walín G. 1985. The thermohaline circulation and the control of ice ages. *Palaeogeogr. Palaeoclimatol. Palaeoecol.* 50: 323–32
- Weaver AJ, Hughes TMC. 1992. Stability and variability of the thermohaline circulation and its link to climate. *Trends Phys. Oceanogr.* 1: 15–70
- Weaver AJ, Sarachik ES. 1990. On the importance of vertical resolution in certain ocean general circulation models. *J. Phys. Oceanogr.* 20: 600–9
- Weaver A, Sarachik ES. 1991. The role of mixed boundary conditions in numerical models of the ocean. *J. Phys. Oceanogr.* 21: 1470–93
- Welander P. 1959. An advective model of the ocean thermocline. *Tellus* 11: 309–18
- Welander P. 1967. On the oscillatory instability of a differentially heated fluid loop. *J. Fluid Mech.* 29: 17–30
- Welander P. 1971. The thermocline problem. *Philos. Trans. R. Soc. London Ser. A* 270: 415–21
- Welander P. 1982. A simple heat-salt oscillator. *Dyn. Atmos. Oceans* 6: 233–42
- Welander P. 1986. Thermohaline effects in the ocean circulation and related simple models. In *Large-Scale Transport Processes in Oceans and Atmosphere*, ed. J. Willebrand, DLT Anderson, pp. 163–200. Dordrecht: Reidel
- Welander P. 1989. A new type of double-diffusive instability? *Tellus* 41A: 66–72
- Whitehead JA. 1991. Small and mesoscale convection as observed in the laboratory. In *Deep Convection and Deep Water Formation in the Oceans*, ed. PC Chu, JC Gascard, pp. 355–68. New York: Elsevier
- Wright DG, Stocker TF. 1991. A zonally averaged ocean model for the thermohaline circulation, Part I: Model development and flow dynamics. *J. Phys. Oceanogr.* 21: 1713–24